Analysis of x-ray polarization to determine the three-dimensionally anisotropic velocity distributions of hot electrons in plasma produced by ultrahigh intensity lasers

Y. Inubushi,* T. Kai, T. Nakamura, S. Fujioka, H. Nishimura, and K. Mima
Institute of Laser Engineering, Osaka University, 2-6 Yamada-oka, Suita, Osaka 565-0871, Japan
(Received 25 October 2006; published 1 February 2007)

A new polarization spectroscopy model has been developed to analyze energetic electrons distributed in a three-dimensional phase space. This model calculates the polarization degrees for a given line of sight. Time-dependent polarization degrees of Heα line emitted from heliumlike chlorine ions was obtained for two different lines of sight by using three-dimensional electron velocity distributions provided with two-dimensional particle-in-cell simulations. These results demonstrate that the polarization degrees are sensitively dependent on the profile of the electron velocity distributions which are affected by the polarization of the laser pulse.

DOI: 10.1103/PhysRevE.75.026401 PACS number(s): 52.70.La, 52.38.Ph

I. INTRODUCTION

Recent advances in ultra-short pulse, high-intensity lasers have opened up possibility of performing unique experiments in fields such as fast ignitor [1,2], particle acceleration [3–6], and short pulse x-ray generation [7]. Efficient energy transport from laser to dense plasma is a critical issue for all of these applications. There are two kinds of electrons in plasmas generated by ultrahigh intensity lasers, namely hot electrons and cold bulk electrons. Hot electrons transfer absorbed laser energy to high-density region of plasma and are predominantly generated by collective processes in the laser-plasma interaction region [8]. Consequently, initial velocity distributions of hot electrons are highly anisotropic. Cold bulk electrons form a return current as a counter stream for hot electrons, and gain energy mostly via the Ohmic process [9]. Thus, velocity distributions of cold electrons are substantially isotropic. Investigation of the velocity distribution function (VDF) of hot electrons is critical for clarifying energy transport by these electrons in ultrahigh intensity laser-produced plasmas.

X-ray polarization spectroscopy is a useful diagnostic tool for measuring the VDF of electrons. In general, polarized radiation is emitted due to anisotropic electron velocity distributions or an anisotropic electromagnetic field [10–12]. By utilizing this principle, the anisotropy of hot electron VDFs can be determined by observing the polarization degree P [13–15]. In the case of a planar target irradiated by a high intensity ($10^{16}-10^{17}$ W/cm^2) laser pulse, hot electrons are predominantly generated by resonance absorption and/or parametric processes so that they initially propagate parallel to the density gradient (i.e., perpendicular to the target surface). This direction is referred to as the quantization axis hereinafter. The observed polarization degree P is defined as

$$P = \frac{I - I_\perp}{I + I_\perp}, \tag{1}$$

where $I_\parallel$ and $I_\perp$ are respectively the intensities of the x-ray radiation whose electric fields are parallel and perpendicular to the quantization axis for an observer. This definition accords with that employed by polarization spectroscopy that uses an electron beam ion trap [16].

The polarization degree is evaluated using axially symmetric VDFs in a conventional way of polarization spectroscopy [13–15,17–19]. Detailed analysis using a kinetics atomic code involved only "beam" electrons [20]. However, electron VDFs in laser-produced plasmas generally have three-dimensional (3D) velocity components which are affected by the polarization of laser pulse. In Ref. [19], though electron VDFs relative to the polarization of the laser were investigated by changing the polarization of the ps-KrF laser, this analysis was performed using the model for axially symmetric VDFs. Treating 3D electron VDFs is necessary to evaluate exactly the alignment generated by anisotropic electrons in laser-produced plasma. In this study, a new polarization spectroscopy model that treats 3D electron VDFs has been developed, and observation of the Cl-Heα line due to the $1s^2{}^1S_0$-$1s2p^1P_1$ transition of a heliumlike chlorine ion is proposed. This model is based on the radiative transition between two energy levels of heliumlike chlorine. Chlorine was selected since the x-ray polarization measurements were performed using a chlorinated plastic target irradiated by a fs-laser pulse [17].

II. POLARIZATION MODEL FOR 3D PHASE SPACE

When an electron beam collides with ions, polarized x rays are emitted. Radiation of π component, the electric field of which is parallel to the electron beam, is emitted by transitions for which there is no change in the magnetic quantum number (i.e., $\Delta M=0$), while radiation of σ component, the electric field of which is perpendicular to the electron beam, is emitted by transitions for which $\Delta M=\pm 1$. In this model, the polarization degree for the Heα line is given by [21]

$$P_0(E)\frac{\sigma_0(E) - \sigma_1(E)}{\sigma_0(E) + \sigma_1(E)}, \tag{2}$$

where $\sigma_i(E)$ is the integral cross sections for the $1s^2{}^1S_0$-$1s2p^1P_1$ transition and it is dependent on the electron impact energy E. The subscript i denotes the magnetic quantum number in the $1s2p^1P_1$ level.

*Email address: yinubusi@ile.osaka-u.ac.jp

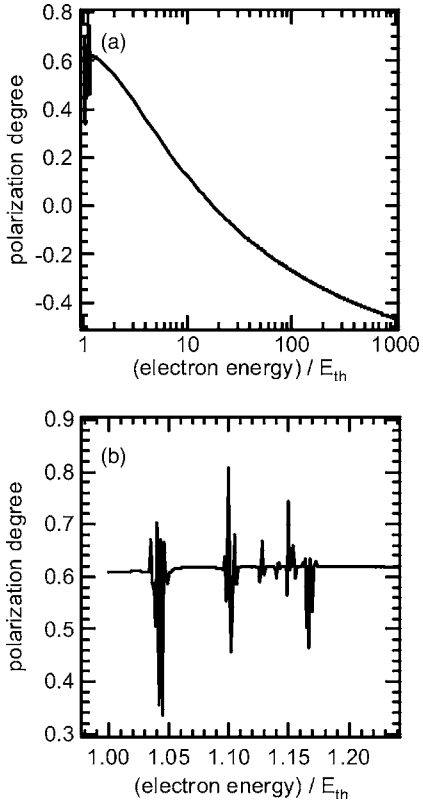

FIG. 1. Polarization degree of Cl-Heα line as a function of electron energy normalized using the threshold energy (2.79 keV) (a) in the high energy region, and (b) near the threshold energy.

The polarization degree can be adequately calculated using a semirelativistic calculation that employs a close-coupling expansion for the ions under consideration [22]. However, a fully relativistic calculation is preferable for the case of highly charged ions [23]. Therefore, the integral cross sections with sublevels were calculated using the semirelativistic Breit-Pauli R-matrix method [24] for the 17 lowest excited levels. In order to obtain the integral cross sections in high-energy region, we fit the present integral cross sections in the high-energy region to each of analytic functions [25]. Figure 1 shows the calculated polarization degree as a function of the energy of the electrons colliding with the He-like chlorine ions. The electron energies are normalized using the threshold energy of the Cl-Heα line (2.79 keV). Figure 1(a) shows the polarization degree between threshold energy and 1000 times of the threshold energy. The polarization degree decreases monotonically with the incident electron energy. Figure 1(b) shows the polarization degree near the threshold energy. In this region, the resonance phenomena [26] can be seen.

The new model is an extension of the axially symmetric model described in Ref. [13]. In a plasma, radiation of polarized x rays are emitted as a result of the alignment generated by electron-ion impacts. This model, which involves only two energy levels ($1s^2\,{}^1S_0$-$1s2p\,{}^1P_1$), exactly treats the generation of the alignment in plasmas considering electron VDFs in 3D phase space. The generated alignment is influenced by various atomic processes such as elastic impact, recombination, and the cascade effect. In the case of dense

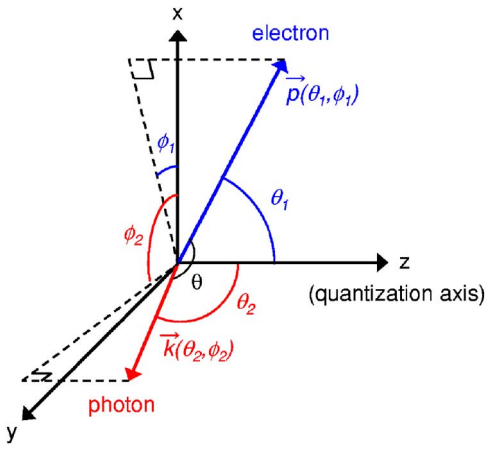

FIG. 2. (Color online) Geometry of the electron-ion impact and photon emission. The z-axis is the quantization axis. $\boldsymbol{p}(\theta_1,\phi_1)$ and $\boldsymbol{k}(\theta_2,\phi_2)$ are the momentum vector of the impact electron and the emitted photon, respectively.

plasmas, such as laser driven implosion cores, it is necessary to use an atomic kinetic code connected with this model, because collisions would probably reduce the polarization degree above critical densities. Therefore this model is valid for low density plasmas such as expanding plasmas from solid targets.

Figure 2 shows the geometry of the electron-ion impact and the photon emission assumed in the model. The z axis is defined as the quantization axis (z). $\boldsymbol{p}(\theta_1,\phi_1)$ and $\boldsymbol{k}(\theta_2,\phi_2)$ are the momentum vector of the impact electron and that of the emitted photon, respectively. During the electric dipole radiation process caused by the electron-ion impact, the angular distributions of the Stokes parameters, I and Q, are given by

$$I(\theta,E)=\frac{3I_0(E)}{4\pi[3-P_0(E)]}[1-P_0(E)\cos^2\theta], \tag{3}$$

and

$$Q(\theta,E)=\frac{3I_0(E)}{4\pi[3-P_0(E)]}P_0(E)\sin^2\theta, \tag{4}$$

where θ is the angle between $\boldsymbol{p}$ and $\boldsymbol{k}$. They are dependent on the angle θ_1, θ_1, ϕ_2, and ϕ_2

$$\cos\theta=\frac{\mathbf{p}(\theta_1,\phi_1)\cdot\mathbf{k}(\theta_2,\phi_2)}{|\mathbf{p}(\theta_1,\phi_1)||\mathbf{k}(\theta_2,\phi_2)|}. \tag{5}$$

The total intensity $I_0(E)$ is given by $I_0(E)=\sqrt{E}\sigma(E)=\sqrt{E}[\sigma_0(E)+2\sigma_1(E)]$. The Stokes parameters of photons emitted from the plasma are given in Eqs. (6) and (7), which take into account the electron energy distribution $f(\theta_1,\phi_1,E)$

$$I'(\theta_2,\phi_2)=\int_{E_{th}}^{\infty}\int_0^{\pi}\int_0^{2\pi}I(\theta,E)f(\theta_1,\phi_1,E)\sin\theta_1 d\phi_1 d\theta_1 dE, \tag{6}$$

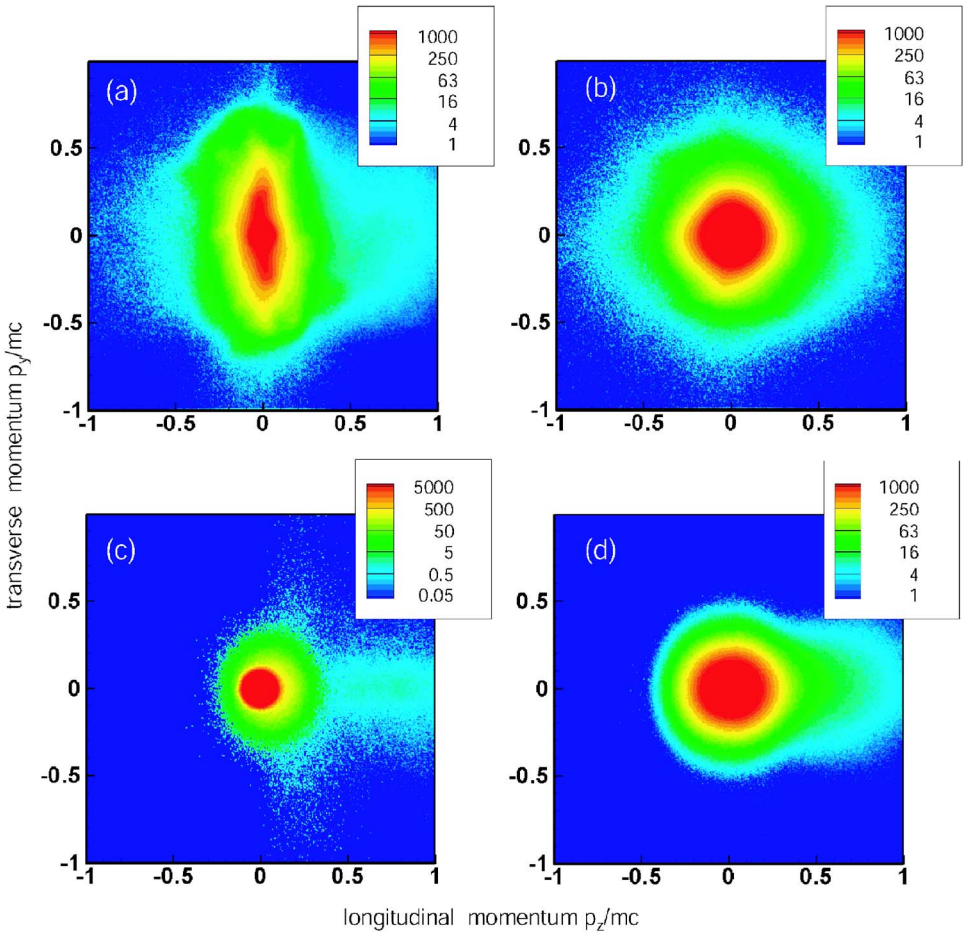

FIG. 3. (Color online) Electron momentum distributions in v_y-v_z space in the interaction region (a) during laser irradiation, (b) after laser irradiation, and in the over dense region (c) during laser irradiation, (d) after laser irradiation.

$$Q'(\theta_2,\phi_2) = \int_{E_{th}}^{\infty}\int_0^{\pi}\int_0^{2\pi} Q(\theta,E) f(\theta_1,\phi_1,E) \times \cos(2\psi)\sin\theta_1 d\phi_1 d\theta_1 dE, \quad (7)$$

where Ψ is the angle between the $\boldsymbol{k}$-z plane and the $\boldsymbol{k}$-$\boldsymbol{p}$ plane

$$\cos\psi = \frac{[\mathbf{z}\times\mathbf{k}(\theta_2,\phi_2)]\cdot[\mathbf{p}(\theta_1,\phi_1)\times\mathbf{k}(\theta_2,\phi_2)]}{|\mathbf{z}\times\mathbf{k}(\theta_2,\phi_2)||\mathbf{p}(\theta_1,\phi_1)\times\mathbf{k}(\theta_2,\phi_2)|}. \quad (8)$$

From the equations above, the polarization degree relative to the line of sight is obtained as

$$P(\theta_2,\phi_2) = \frac{Q'(\theta_2,\phi_2)}{I'(\theta_2,\phi_2)}. \quad (9)$$

III. CALCULATION AND DISCUSSION

In the model calculation, the electron distribution was derived using a two-dimensional (2D) particle-in-cell (PIC) simulation. This simulation calculates the VDF in 2D planes (y, z) and 3D phase spaces (v_x, v_y, v_z). The dimensions of the system were 11.5 μm by 25 μm. The target is assumed to consist of electrons having an initial temperature of 500 eV and immobile ions. The density profile of the target had a profile that was 100 times greater than the critical density n_c for a 1 μm wavelength laser with exponentially decreasing preformed plasma of 3 μm scale length. A p-polarized 1 μm wavelength laser pulse with 130 fs duration irradiates the target at 5° incidence with respect to the target normal. The laser ramps up in a 5 laser cycle and keeps the peak intensity of 1.3×10^{17} W/cm^2. The laser irradiance is uniform in the y direction. The boundary conditions are periodic in the y direction, and absorbing in the z direction. The plane of the laser polarization is the $y-z$ plane. This PIC simulation calculated the time-dependent electron VDFs in the laser-plasma interaction region and in the over dense region.

Figure 3 show the electron momentum distributions in v_y-v_z space in the laser-plasma interaction region and in the over dense region. Figure 4 shows the calculated time-dependent polarization degrees around the critical point and the point of $4n_c$ relative to the line of sight in the vicinity of the x axis ($\theta_2=95°$ and $\phi_2=0°$). These are calculated directly by substituting the PIC simulation results for $f(\theta_1,\phi_1,E)$ into Eqs. (7)–(9). In the laser-plasma interaction region, the polarization degrees are negative during laser irradiation. These values are caused by the electrons quivering in electric field of the laser as shown in Fig. 3(a). After the laser pulse has stopped, this quivering motion disappears [Fig. 3(b)] and the polarization degree increases until it saturates at about 0.2. In the over dense region, during laser irradiation, high energy electrons are accelerated in the forward direction [Fig. 3(c)], and the polarization degree decreases because the electron energies reach sufficiently high levels to produce a negative polarization degree as shown in Fig. 1. At later times, the

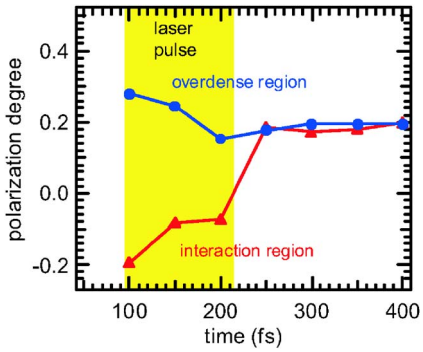

FIG. 4. (Color online) Time-dependent polarization degrees relative to the line of sight in the vicinity of the x axis (θ_2=95° and ϕ_2=0°) in the interaction region (around the critical point) and in the over dense region (around the point of $4n_c$). The yellow section represents the period that the laser pulse was on.

angular distribution of the hot electrons broadens [Fig. 3(d)], and the polarization degree increase slightly and becomes steady as well as that in the interaction region.

Figure 5 shows the electron momentum distributions in the v_x–v_z space, and Fig. 6 shows the calculated time-dependent polarization degrees around the critical point and around the point of $4n_c$ relative to the line of sight in the vicinity of the y axis (θ_2=95° and ϕ_2=90°). In the laser-plasma interaction region, the polarization degrees during laser irradiation are lower than those after laser irradiation because the energy of electrons moving along the z axis declines with time as shown in Figs. 5(a) and 5(b). In the over dense region during laser irradiation, high energy electrons are accelerated only in the forward direction [Fig. 5(c)]. After the laser irradiation, the momentum distribution and the polarization degrees are steady at around 0.4 as well as those of the interaction region.

Experimentally measured time-integrated polarization degrees of the Cl-Heα line are reported in Ref. [17]. The conditions of this experiment are similar to those used in the PIC simulation. The experimental plasma is optically thin for the Cl-Heα line, which was confirmed by calculating the averaged charge state of the chlorine ions using the FLY code [27]. In the experiment the line of sight was θ_2=95° and ϕ_2=90°. Therefore the experimentally measured polarization degrees are compared with the calculated results shown in Fig. 6. The experimentally measured polarization degrees were $-0.07^{+0.052}_{-0.047}$ in the interaction region and $0.32^{+0.071}_{-0.10}$ in the over dense region. The calculated polarization degrees and the experimental results both show that the polarization degree in the over dense region is higher than that in the interaction region showing a qualitative agreement between them. In the over dense region the value of experimentally measured polarization degree is in good agreement with the calculation results. However, in interaction region the calculated polarization degrees are higher than the experimental value. The plausible reason for this disagreement will be the

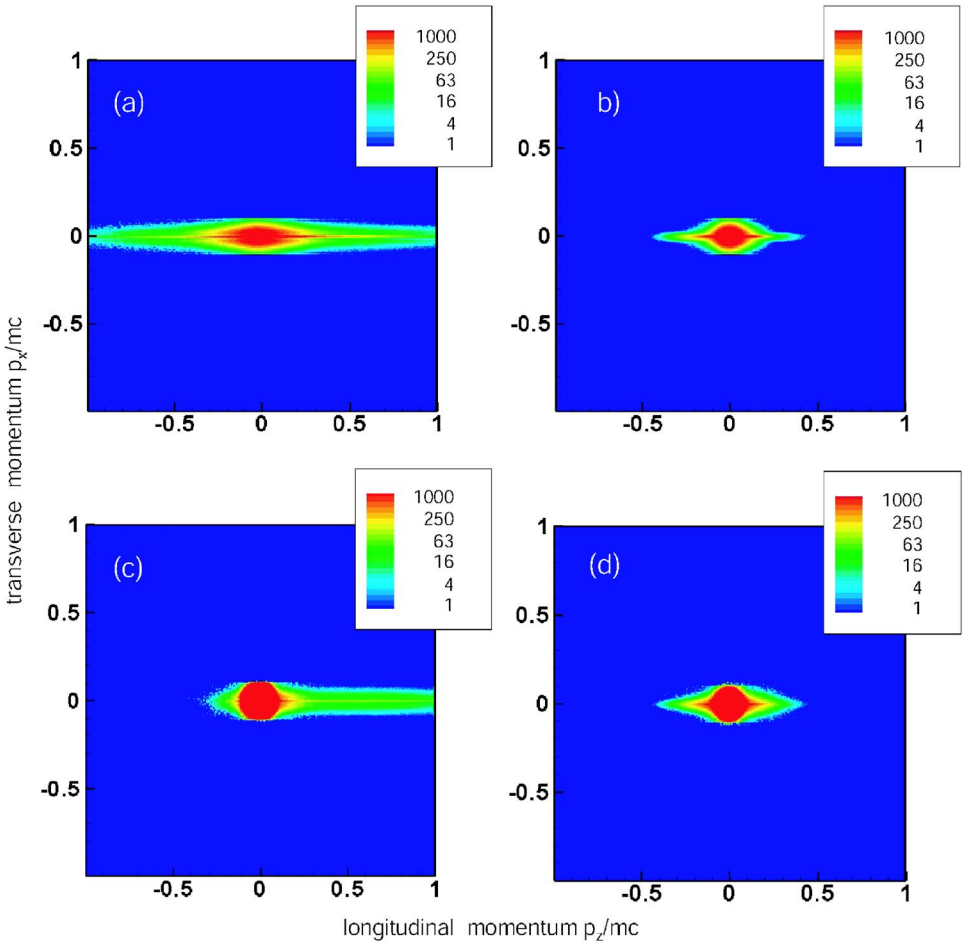

FIG. 5. (Color online) Electron momentum distributions in the v_x–v_z space in the interaction region (a) during laser irradiation, (b) after laser irradiation, and in the over dense region (c) during laser irradiation, (d) after laser irradiation.

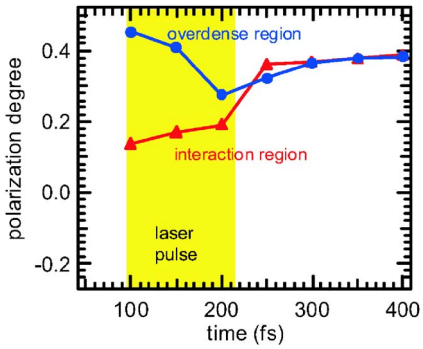

FIG. 6. (Color online) Time-dependent polarization degrees observed from the line of sight near the y axis (θ_2=95° and ϕ_2=90°) in the interaction region (around the critical point) and in the over dense region (around the point of $4n_c$). The yellow section represents the period that the laser pulse was on.

angular spread of incident laser onto the target. The cone-half angle of the incident laser used in the experiment was 9°. This focusing profile of the laser is not included in the present 2D PIC simulation. A PIC simulation treating this laser incident angle is of importance to validate the model prediction and comparison with experiments. Furthermore, if it were possible to obtain time-resolved measurements of polarization spectroscopy, it should be possible to quantitatively understand energy transport in an ultrahigh intensity laser proposed plasma.

IV. CONCLUSION

A new polarization spectroscopy model has been developed to diagnose the 3D electron VDF in an ultrahigh intensity laser produced plasma. It is shown that the polarization degrees are strongly dependent on the electron VDF and agree qualitatively with the experimental results. Treatment of 3D electron VDFs for detailed analysis combined with atomic kinetic code is essential for x-ray polarization spectroscopy in laser produced plasma. The model suggested in this study is simple and useful for diagnosing electron VDFs in low density plasmas.

ACKNOWLEDGMENTS

The authors would like to thank T. Kawamura and T. Johzaki for their support and for many helpful discussions. This work was partly supported by MEXT, Grant-in Aid for Creative Scientific Research (15GS0214).

[1] M. Tabak, J. Hammer, M. E. Glinsky, W. L. Kruer, S. C. Wilks, J. Woodworth, E. M. Cambell, M. D. Perry, and R. J. Mason, Phys. Plasmas **1**, 1624 (1994).
[2] R. Kodama, H. Shiraga, K. Shigemori, Y. Tohyama, S. Fujioka, H. Azechi, H. Fujita, H. Habara, T. Hall, Y. Izawa, T. Jitsuno, Y. Kitagawa, K. M. Krushelnick, K. L. Lancaster, K. Mima, K. Nagai, M. Nakai, H. Nishimura, T. Norimatsu, P. A. Norreys, S. Sakabe, K. A. Tanaka, A. Youssef, M. Zept, and T. Yamanaka, Nature (London) **418**, 933 (2002).
[3] T. Tajima and J. M. Dawson, Phys. Rev. Lett. **43**, 267 (1979).
[4] S. P. D. Mangles, C. D. Murphy, Z. Najmudin, A. G. R. Thomas, J. L. Collier, A. E. Dangor, E. J. Divall, P. S. Foster, J. G. Gallacher, C. J. Hooker, D. A. Jaroszynski, A. J. Langley, W. B. Mori, P. A. Norreys, F. S. Tsung, R. Viskup, B. R. Walton-and, and K. Krushelnick, Nature (London) **431**, 535 (2004).
[5] C. G. R. Geddes, C. S. Toth, J. Van Tilborg, E. Esarey, C. B. Schroeder, D. Bruhwiler, C. Nieter, J. Cary, and W. P. Leemans, Nature (London) **431**, 538 (2004).
[6] J. Faure, Y. Glinec, A. Pukhov, S. Kiselev, S. Gordienko, E. Lefebvre, J. P. Rousseau, F. Burgy, and V. Malka, Nature (London) **431**, 541 (2004).
[7] A. Rousse, C. Rischel, S. Fourmaux, I. Uschmann, S. Sebban, G. Grillon, Ph. Balcou, E. Forster, J. P. Geindre, P. Audebert, J. C. Gautheir, and D. Hulin, Nature (London) **410**, 65 (2001).
[8] S. C. Wilks and W. L. Kruer, IEEE J. Quantum Electron. **33**, 1954 (1997), and references therein.
[9] Y. Sentoku, K. Mima, P. Kaw, and K. Nishikawa, Phys. Rev. Lett. **90**, 155001 (2003).
[10] M. Lombardi and J. C. Pebay-peyroula, Acad. Sci., Paris, C. R. **261**, 1485 (1965).
[11] Kh. Kallas and M. Chaika, Opt. Spectra **27**, 376 (1969).
[12] C. G. Carrington and A. Corney, Opt. Commun. **1**, 115 (1969).
[13] E. Haug, Sol. Phys. **71**, 77 (1981).
[14] J. C. Kieffer, J. P. Matte, H. Pepin, M. Chaker, Y. Beaudoin, T. W. Johnston, C. Y. Chien, S. Coe, G. Mourou, and J. Dubau, Phys. Rev. Lett. **68**, 480 (1992).
[15] J. C. Kieffer, J. P. Matte, M. Chaker, Y. Beaudoin, C. Y. Chien, S. Coe, G. Mourou, J. Dubau, and M. K. Inal, Phys. Rev. E **48**, 4648 (1993).
[16] P. Beiersdorfer and M. Slater, Phys. Rev. E **64**, 066408 (2001).
[17] Y. Inubushi, H. Nishimura, M. Ochiai, S. Fujioka, T. Johzaki, K. Mima, T. Kawaura, S. Nakazaki, T. Kai, S. Sakabe, and Y. Izawa, J. Quant. Spectrosc. Radiat. Transf. **99**, 305 (2006); J. Quant. Spectrosc. Radiat. Transf. **101**, 191 (2006).
[18] F. Walden, H.-J. Kunze, A. Petoyan, A. Urnov, and J. Dubau, Phys. Rev. E **59**, 3562 (1999).
[19] H. Yoneda, N. Hasegawa, S. Kawana, and K. I. Ueda, Phys. Rev. E **56**, 988 (1997).
[20] P. Hakel, R. C. Mancini, J. C. Gauthier, E. Minguez, J. Dubau, and M. Cornille, Phys. Rev. E **69**, 056405 (2004).
[21] I. C. Percival and M. J. Seaton, Philos. Trans. R. Soc. London **251**, 113 (1958).
[22] T. Kai, S. Nakazaki, and K. A. Berrington, Nucl. Instrum. Methods Phys. Res. B **235**, 249 (2005).
[23] K. J. Reed and M. H. Chen, Phys. Rev. A **48**, 3644 (1993).
[24] K. A. Berrington, W. B. Eissner, and P. H. Norrington, Comput. Phys. Commun. **92**, 290 (1995).
[25] M. K. Inal and J. Dubau, J. Phys. B **20**, 4221 (1987).
[26] H. Feshbach, Ann. Phys. **5**, 357 (1958).
[27] R. W. Lee and J. T. Larsen, J. Quant. Spectrosc. Radiat. Transf. **56**, 535 (1996).